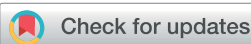


## EDGE ARTICLE

[View Article Online](#)  
[View Journal](#) | [View Issue](#)


Cite this: *Chem. Sci.*, 2020, **11**, 10764

All publication charges for this article have been paid for by the Royal Society of Chemistry

Received 12th March 2020  
Accepted 3rd May 2020

DOI: 10.1039/d0sc01515f  
[rsc.li/chemical-science](http://rsc.li/chemical-science)

*o*-Carboranes, icosahedral carboranes – three-dimensional arene analogues – represent an important class of carbon–boron molecular clusters.<sup>1</sup> The regioselective functionalization of *o*-carboranes has attracted growing interest due to its potential applications in supramolecular design,<sup>2</sup> medicine,<sup>3</sup> optoelectronics,<sup>4</sup> nanomaterials,<sup>5</sup> boron neutron capture therapy agents<sup>6</sup> and organometallic/coordination chemistry.<sup>7</sup> In recent years, transition metal-catalyzed cage B–H activation for the regioselective boron functionalization of *o*-carboranes has emerged as a powerful tool for molecular syntheses. However, the 10 B–H bonds of *o*-carboranes are not equal, and the unique structural motif renders their selective functionalization difficult, since the charge differences are very small and the electrophilic reactivity in unfunctionalized *o*-carboranes reduces in the following order: B(9,12) > B(8,10) > B(4,5,7,11) > B(3,6).<sup>8</sup> Therefore, efficient and selective boron substitution of *o*-carboranes continues to be a major challenge.

Recently, transition metal-catalyzed carboxylic acid or formyl-directed B(4,5)–H functionalization of *o*-carboranes has drawn increasing interest, since it provides an efficient approach for direct regioselective boron–carbon and boron–heteroatom bond formations (Scheme 1a),<sup>9</sup> with major contributions by the groups of Xie,<sup>10</sup> and Yan,<sup>11</sup> among others.<sup>12</sup> Likewise, pyridyl-directed B(3,6)–H acyloxylations (Scheme 1b),<sup>13</sup> and amide-assisted B(4,7,8)–H arylations<sup>14</sup> (Scheme 1c) have been enabled by rhodium or palladium catalysis, respectively.<sup>15,16</sup> Despite indisputable progress, efficient approaches for complementary site-selective functionalizations of *o*-carboranes are hence in high demand.<sup>17</sup> Hence, metal-catalyzed

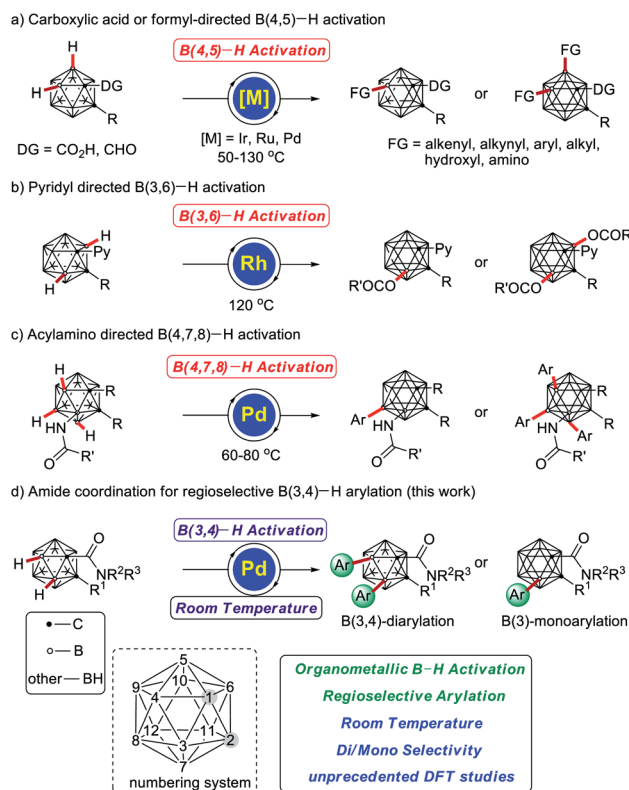
## Regioselective B(3,4)–H arylation of *o*-carboranes by weak amide coordination at room temperature†

Yu-Feng Liang,‡ Long Yang, ID‡ Becky Bongsuiru Jei, Rositha Kuniyil and Lutz Ackermann ID\*

Palladium-catalyzed regioselective di- or mono-arylation of *o*-carboranes was achieved using weakly coordinating amides at room temperature. Therefore, a series of B(3,4)-diarylated and B(3)-monoarylated *o*-carboranes anchored with valuable functional groups were accessed for the first time. This strategy provided an efficient approach for the selective activation of B(3,4)–H bonds for regioselective functionalizations of *o*-carboranes.

position-selective B(3,4)–H functionalizations of *o*-carboranes have thus far not been reported.

Arylated compounds represent key structural motifs in *inter alia* functional materials, biologically active compounds, and natural products.<sup>18</sup> In recent years, transition metal-catalyzed chelation-assisted arylations have received significant attention as environmentally benign and economically superior



Institut für Organische und Biomolekulare Chemie, Georg-August-Universität Göttingen, Tammannstraße 2, 37077 Gottingen, Germany. E-mail: Lutz.Ackermann@chemie.uni-goettingen.de

† Electronic supplementary information (ESI) available. See DOI: 10.1039/d0sc01515f

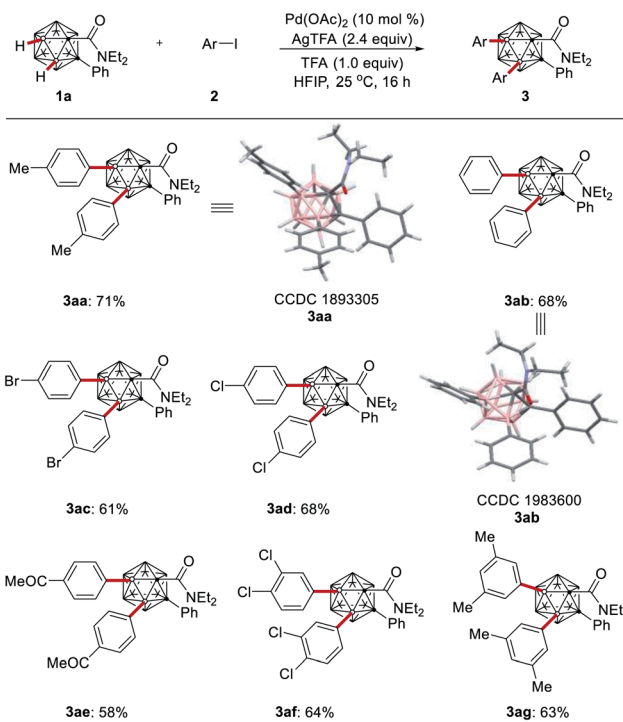
‡ These authors contributed equally to this work.

Scheme 1 Chelation-assisted transition metal-catalyzed cage B–H activation of *o*-carboranes.



alternatives to traditional cross-coupling reactions.<sup>19</sup> Within our program on sustainable C–H activation,<sup>20</sup> we have now devised a protocol for unprecedented cage B–H arylations of *o*-carboranes with weak amide assistance, on which we report herein. Notable features of our findings include (a) transition metal-catalyzed room temperature B–H functionalization, (b) high levels of positional control, delivering B(3,4)-diarylated and B(3)-monoarylated *o*-carboranes, and (c) mechanistic insights from DFT computation providing strong support for selective B–H arylation (Scheme 1d).

We initiated our studies by probing various reaction conditions for the envisioned palladium-catalyzed B–H arylation of *o*-carborane amide **1a** with 1-iodo-4-methylbenzene (**2a**) at room temperature (Tables 1 and S1†). We were delighted to observe that the unexpected B(3,4)-di-arylated product **3aa** was obtained in 59% yield in the presence of 10 mol% Pd(OAc)<sub>2</sub> and 2 equiv. of AgTFA, when HFIP was employed as the solvent, which proved to be the optimal choice (entries 1–5).<sup>21</sup> Control experiments confirmed the essential role of the palladium catalyst and silver additive (entries 6–7). Further optimization revealed that AgOAc, Ag<sub>2</sub>O, K<sub>2</sub>HPO<sub>4</sub>, and Na<sub>2</sub>CO<sub>3</sub> failed to show any beneficial effect (entries 8–11). Increasing the reaction temperature fell short in improving the performance (entries 12 and 13). The replacement of the amide group in substrate **1a** with a carboxylic acid, aldehyde, ketone, or ester group failed to



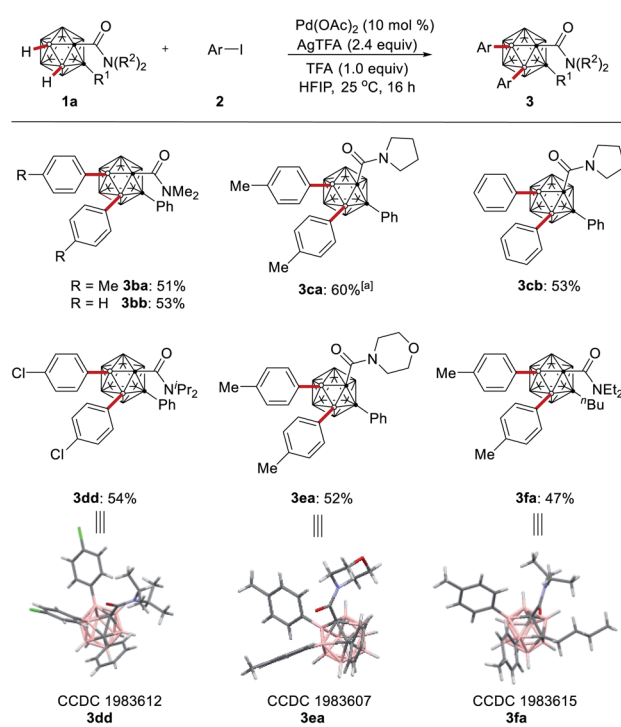
Scheme 2 Cage B(3,4)-H di-arylation of *o*-carboranes.

Table 1 Optimization of reaction conditions<sup>a</sup>

Entry	Additive	Solvent	Yield of <b>3aa</b> /%	Yield of <b>4aa</b> /%
1	AgTFA	PhMe	0	0
2	AgTFA	DCE	0	0
3	AgTFA	1,4-Dioxane	0	0
4	AgTFA	TFE	21	3
5	AgTFA	HFIP	59	4
6	AgTFA	HFIP	0	0 <sup>b</sup>
7	—	HFIP	0	0
8	AgOAc	HFIP	5	<3
9	Ag <sub>2</sub> O	HFIP	<3	<3
10	K <sub>2</sub> HPO <sub>4</sub>	HFIP	0	0
11	Na <sub>2</sub> CO <sub>3</sub>	HFIP	0	0
12	AgTFA	HFIP	53	4 <sup>c</sup>
13	AgTFA	HFIP	42	3 <sup>d</sup>
14	<b>AgTFA</b>	<b>HFIP</b>	<b>71</b>	<3 <sup>e</sup>
15	Ag <sub>2</sub> CO <sub>3</sub>	HFIP	9	34 <sup>f</sup>
16	Ag <sub>2</sub> CO <sub>3</sub>	HFIP	5	55 <sup>f,g</sup>

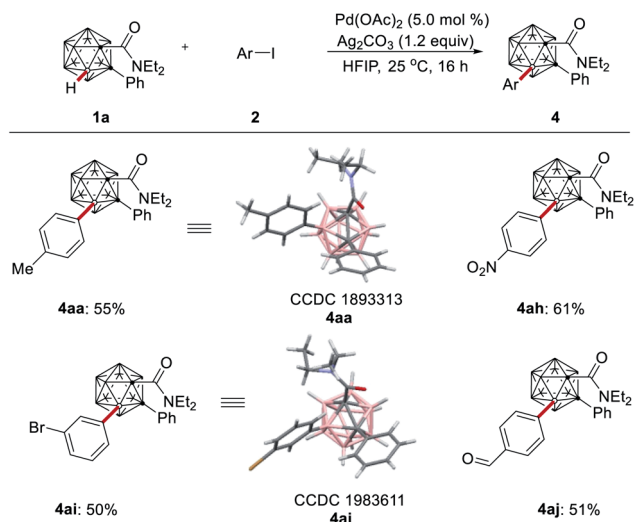
<sup>a</sup> Reaction conditions: **1a** (0.20 mmol), **2** (0.48 mmol), Pd(OAc)<sub>2</sub> (10 mol%), additive (0.48 mmol), solvent (0.50 mL), 25 °C, 16 h, and isolated yield. <sup>b</sup> Without Pd(OAc)<sub>2</sub>. <sup>c</sup> At 40 °C. <sup>d</sup> At 60 °C. <sup>e</sup> TFA (0.2 mmol) was added. <sup>f</sup> **1a** (0.20 mmol), **2a** (0.24 mmol), Pd(OAc)<sub>2</sub> (5.0 mol%), and Ag<sub>2</sub>CO<sub>3</sub> (0.24 mmol). <sup>g</sup> **2a** was added in three portions every 4 h. DCE = dichloroethane, TFE = 2,2-trifluoroethanol, HFIP = hexafluoroisopropanol, and TFA = trifluoroacetic acid.

afford the desired arylation product (see the ESI†). We were pleased to find that the use of 1.0 equiv. of trifluoroacetic acid (TFA) as an additive improved the yield to 71% (entry 14). To our delight, replacing the silver additive with Ag<sub>2</sub>CO<sub>3</sub> resulted in the



Scheme 3 Effect of substituents on B–H diarylation. <sup>a</sup>At 50 °C.

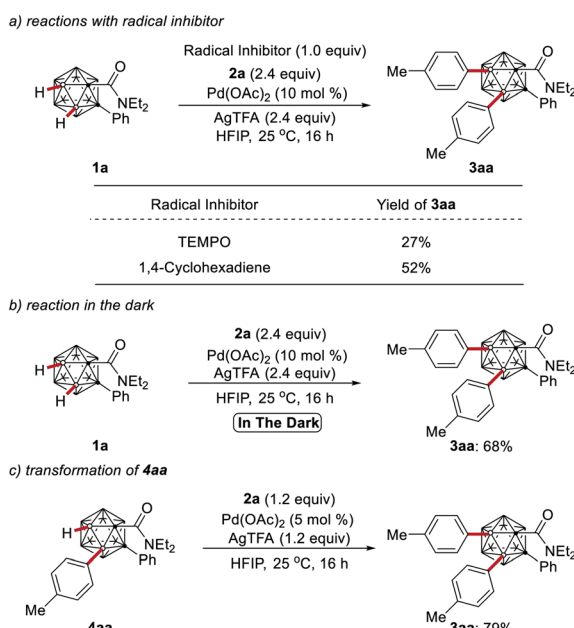




formation of B(3)-H mono-arylation product **4aa** as the major product (entries 15–16).

With the optimized reaction conditions in hand, we probed the scope of the B-H di-arylation of *o*-carboranes **1a** with different aryl iodides **2** (Scheme 2). The versatility of the room temperature B(3,4)-H di-arylation was reflected by tolerating valuable functional groups, including bromo, chloro, and enolizable ketone substituents. The connectivity of the products **3aa** and **3ab** was unambiguously verified by X-ray single crystal diffraction analysis.<sup>22</sup>

Next, we explored the effect exerted by the *N*-substituent at the amide moiety (Scheme 3). Tertiary amides **1b–1f** proved to be suitable substrates with optimal results being accomplished with substrate **1a**. The effect of varying the cage carbon



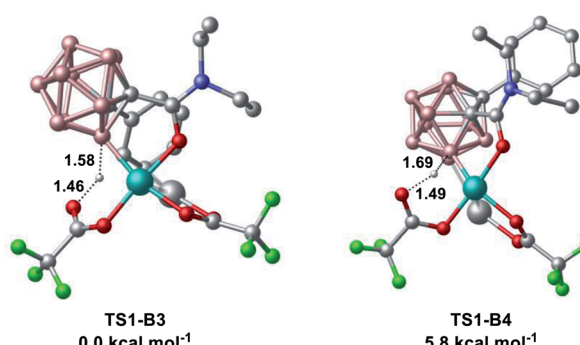
**Scheme 5** Control experiments.

substituents R<sup>1</sup> on the reaction's outcome was also probed, and both aryl and alkyl substituents gave the B-H arylation products and the molecular structures of the products **3dd**, **3ea** and **3fa** were fully established by single-crystal X-ray diffraction.

The robustness of the palladium-catalyzed B-H functionalization was subsequently investigated for the challenging catalytic B-H monoarylation of *o*-carboranes (Scheme 4). The B(3)-H monoarylation, as confirmed by single-crystal X-ray diffraction analysis of products **4aa** and **4ai**, proceeded smoothly with valuable functional groups, featuring aldehyde and nitro substituents, which should prove invaluable for further late-stage manipulation.

To elucidate the palladium catalysts' working mode, a series of experiments was performed. The reactions in the presence of TEMPO or 1,4-cyclohexadiene produced the desired product **3aa**, which indicates that the present B-H arylation is less likely to operate *via* radical intermediates (Scheme 5a). The palladium catalysis carried out in the dark performed efficiently (Scheme 5b). Compound **4aa** could be converted to di-arylation product

**a) First B-H activation transition states at the B3 and B4 positions**



**b) Second B-H activation transition states at the B4 and B6 positions**

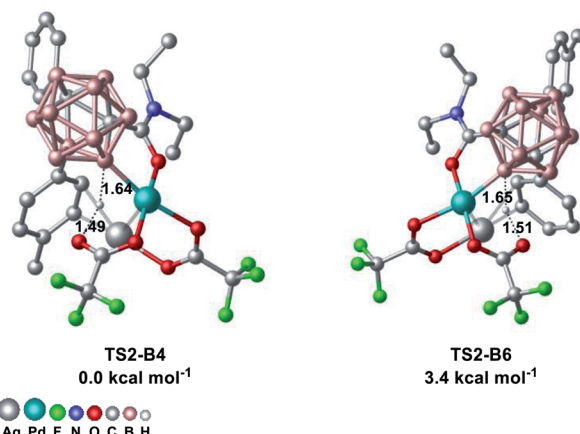


**Fig. 1** Computed relative Gibbs free energies in kcal mol<sup>-1</sup> and the optimized geometries of the transition states involved in the B-H activation at the PBE0-D3(BJ)/def2-TZVP+SMD(HFIP)/TPSS-D3(BJ)/def2-SVP level of theory. (a) First B-H activation transition states at the B3 and B4 positions. (b) Second B-H activation transition states at the B4 and B6 positions. Irrelevant hydrogen atoms in the transition states are omitted for clarity and the bond lengths are given in Å.



**3aa** with high efficiency, indicating that **4aa** is an intermediate for the formation of the diarylated cage **3aa** (Scheme 5c).

To further understand the catalyst mode of action, we studied the site-selectivity of the *o*-carborane B–H activation for the first B–H activation at the B3 *versus* B4 position and for the second B–H activation at the B4 *versus* B6 position using density functional theory (DFT) at the PBE0-D3(BJ)/def2-TZVP+SMDFIP(TPSS-D3(BJ)/def2-SVP level of theory (Fig. 1). Our computational studies show that the B3 position is 5.8 kcal mol<sup>-1</sup> more favorable than the B4 position for the first B–H activation, while the B4 position is 3.4 kcal mol<sup>-1</sup> more favorable than the B6 position for the second B–H activation. It is noteworthy that here the interaction between AgTFA and a cationic palladium(II) complex was the key to success, being in good agreement with our experimental results (for more details, see the ESI†).

A plausible reaction mechanism is proposed which commences with an organometallic B(3)–H activation of **1a** with weak assistance of the amide group and assistance by AgTFA to form the cationic intermediate **I** (Scheme 6). Oxidative addition with the aryl iodide **2** affords the proposed cationic palladium(IV) intermediate **II**, followed by reductive elimination to give the B(3)-mono-arylation product **4aa**. Subsequent B(4)-arylation occurs assisted by the weakly coordinating amide to generate the B(3,4)-di-arylation product **3aa**. Due to the innate higher reactivity of the B(4)–H bond in intermediate **4aa** – which is inherently higher than that of the B(6)–H bond – the B(3,6)-arylation product is not formed.

In summary, room temperature palladium-catalyzed direct arylations at cage B(3,4) positions in *o*-carboranes have been achieved with the aid of weakly coordinating, synthetically useful amides. Thus, palladium-catalyzed B–H activations enable the assembly of a wealth of arylated *o*-carboranes. This method features high site-selectivity, high tolerance for

functional groups, and mild reaction conditions, thereby offering a platform for the design and synthesis of boron-substituted *o*-carboranes. Our findings offer a facile strategy for selective activations of B(3,4)–H bonds, which will be instrumental for future design of optoelectronics, nanomaterials, and boron neutron capture therapy agents.

## Conflicts of interest

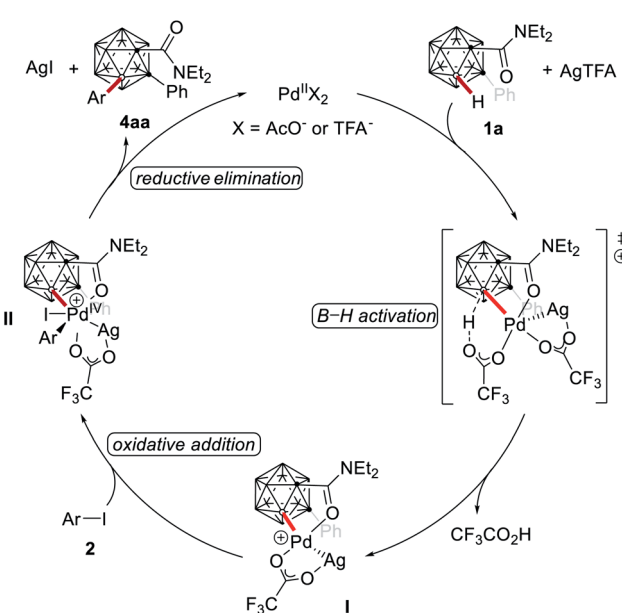
There are no conflicts to declare.

## Acknowledgements

Generous support by the Alexander von Humboldt Foundation (fellowship to Y. L.), the CSC (fellowship to L. Y.), the DAAD (fellowship to B. B. J.) and the DFG (Gottfried-Wilhelm-Leibniz prize to L. A.) is gratefully acknowledged. We also thank Dr J. Li for donation of chemicals and Dr Christopher Golz (University Göttingen) for support with the X-ray diffraction analysis.

## Notes and references

- (a) R. N. Grimes, *Carboranes*, Academic Press, Amsterdam, 3rd edn, 2016; (b) Z. Xie and G.-X. Jin, *Dalton Trans.*, 2014, **43**, 4924–5133; (c) J. Poater, M. Solà, C. Viñas and F. Teixidor, *Angew. Chem., Int. Ed.*, 2014, **53**, 12191–12195; (d) N. S. Hosmane, *Boron Science: New Technologies and Applications*, Taylor & Francis Books/CRC Press, Boca Raton, FL, 2012.
- (a) J. J. Schwartz, A. M. Mendoza, N. Wattanatorn, Y. Zhao, V. T. Nguyen, A. M. Spokoyny, C. A. Mirkin, T. Baše and P. S. Weiss, *J. Am. Chem. Soc.*, 2016, **138**, 5957–5967; (b) R. N. Grimes, *Dalton Trans.*, 2015, **44**, 5939–5956; (c) D. Brusselle, P. Bauduin, L. Girard, A. Zaulet, C. Viñas, F. Teixidor, I. Ly and O. Diat, *Angew. Chem., Int. Ed.*, 2013, **52**, 12114–12118; (d) A. M. Cioran, A. D. Musteti, F. Teixidor, Ž. Krpetić, I. A. Prior, Q. He, C. J. Kiely, M. Brust and C. Viñas, *J. Am. Chem. Soc.*, 2012, **134**, 212–221; (e) P. Bauduin, S. Prevost, P. Farràs, F. Teixidor, O. Diat and T. Zemb, *Angew. Chem., Int. Ed.*, 2011, **50**, 5298–5300; (f) B. P. Dash, R. Satapathy, E. R. Gaillard, J. A. Maguire and N. S. Hosmane, *J. Am. Chem. Soc.*, 2010, **132**, 6578–6587.
- (a) Z. J. Leśnikowski, *J. Med. Chem.*, 2016, **59**, 7738–7758; (b) F. Issa, M. Kassiou and L. M. Rendina, *Chem. Rev.*, 2011, **111**, 5701–5722; (c) M. Scholz and E. Hey-Hawkins, *Chem. Rev.*, 2011, **111**, 7035–7062.
- (a) S. Mukherjee and P. Thilagar, *Chem. Commun.*, 2016, **52**, 1070–1093; (b) R. Núñez, M. Tarrés, A. Ferrer-Ugalde, F. F. de Biani and F. Teixidor, *Chem. Rev.*, 2016, **116**, 14307–14378; (c) X. Li, H. Yan and Q. Zhao, *Chem.-Eur. J.*, 2016, **22**, 1888–1898.
- (a) E. Q. Qian, A. I. Wixstrom, J. C. Axtell, A. Saebi, P. Rehak, Y. Han, E. H. Mouly, D. Mosallaei, S. Chow, M. Messina, J.-Y. Wang, A. T. Royappa, A. L. Rheingold, H. D. Maynard, P. Kral and A. M. Spokoyny, *Nat. Chem.*, 2017, **9**, 333–340; (b) A. Saha, E. Oleshkevich, C. Viñas and F. Teixidor, *Adv.*



Scheme 6 Proposed reaction mechanism.





- 5, 91683–91685; (o) Y. Quan, Z. Qiu and Z. Xie, *J. Am. Chem. Soc.*, 2014, **136**, 7599–7602; (p) Z. Qiu, Y. Quan and Z. Xie, *J. Am. Chem. Soc.*, 2013, **135**, 12192–12195.
- 18 (a) M. Seki, *Org. Process Res. Dev.*, 2016, **20**, 867–877; (b) J. Hubrich, T. Himmeler, L. Rodefeld and L. Ackermann, *ACS Catal.*, 2015, **5**, 4089–4093; (c) D. A. Horton, G. T. Bourne and M. L. Smythe, *Chem. Rev.*, 2003, **103**, 893–930.
- 19 Selected reviews: (a) S. Rej, Y. Ano and N. Chatani, *Chem. Rev.*, 2020, **120**, 1710–1787; (b) P. Gandeepan, T. Muller, D. Zell, G. Cera, S. Warratz and L. Ackermann, *Chem. Rev.*, 2019, **119**, 2192–2452; (c) J. C. K. Chu and T. Rovis, *Angew. Chem., Int. Ed.*, 2018, **57**, 62–101; (d) P. Gandeepan and L. Ackermann, *Chem.*, 2018, **4**, 199–222; (e) Y. Park, Y. Kim and S. Chang, *Chem. Rev.*, 2017, **117**, 9247–9301; (f) D.-S. Kim, W.-J. Park and C.-H. Jun, *Chem. Rev.*, 2017, **117**, 8977–9015; (g) Z. Dong, Z. Ren, S. J. Thompson, Y. Xu and G. Dong, *Chem. Rev.*, 2017, **117**, 9333–9403; (h) R.-Y. Zhu, M. E. Farmer, Y.-Q. Chen and J.-Q. Yu, *Angew. Chem., Int. Ed.*, 2016, **55**, 10578–10599; (i) T. Gensch, M. N. Hopkinson, F. Glorius and J. Wencel-Delord, *Chem. Soc. Rev.*, 2016, **45**, 2900–2936; (j) K. Hirano and M. Miura, *Chem. Lett.*, 2015, **44**, 868–873; (k) D. A. Colby, A. S. Tsai, R. G. Bergman and J. A. Ellman, *Acc. Chem. Res.*, 2012, **45**, 814–825; (l) T. Satoh and M. Miura, *Chem.–Eur. J.*, 2010, **16**, 11212–11222.
- 20 (a) L. Ackermann, *Acc. Chem. Res.*, 2020, **53**, 84–104; (b) J. Loup, U. Dhawa, F. Pesciaioli, J. Wencel-Delord and L. Ackermann, *Angew. Chem., Int. Ed.*, 2019, **58**, 12803–12818; (c) L. Ackermann, *Acc. Chem. Res.*, 2014, **47**, 281–295.
- 21 J. Wencel-Delord and F. Glorius, *Nat. Chem.*, 2013, **5**, 369–375.
- 22 CCDC 1893305 (**3aa**), 1983600 (**3ab**), 1983612 (**3dd**), 1983607 (**3ea**), 1983615 (**3fa**), 1893313 (**4aa**) and 1983611 (**4ai**) contain the supplementary crystallographic data.

